ACADEMIA ROMÂNĂ
Revue Roumaine de Chimie
http://web.icf.ro/rrch/

Rev. Roum. Chim.,
2021, *66*(10-11), 813–818
DOI: 10.33224/rrch.2021.66.10-11.04

Dedicated to the memory of
Prof. Petre T. FRANGOPOL (1933-2020)

IS THE NET ELECTRIC CHARGE INJECTED INTO A CELL THE ONLY DRIVER OF ITS RESPONSE?

Davy C. VANDERWEYEN, Derek R. TUCK and Sorinel A. OPRISAN

Department of Physics and Astronomy, College of Charleston, 66 George Street, Charleston, SC~29424, U.S.A.

Received June 25, 2021

A widely accepted tenet in neuroscience is that excitable cells, such as neurons, cardiac, and pancreatic cells, respond to external stimuli by producing significant all-or-nothing stereotypical electrical impulses called action potentials (APs). The characteristics of the external stimuli, such as their intensity (amplitude) or duration and their relative timing (or phase) relative to the most recent AP, are encoded in transient changes of the firing frequency of the afferent neuron(s). We used a single-compartment, Hodgkin-Huxley type, model neuron to investigate numerically neurons' responses to stimuli. Our results indicate that the total amount of injected electric charge, determined by the amplitude (intensity) and duration of the stimulus, is the primary driver of transient changes in the firing period of neurons. We also find that while the neurons' response is linear with stimulus amplitude, it has a robust nonlinear behavior with respect to stimulus duration. Furthermore, we found that neurons are sensitive to the stimulus shape, not only to the total area of the stimulus.

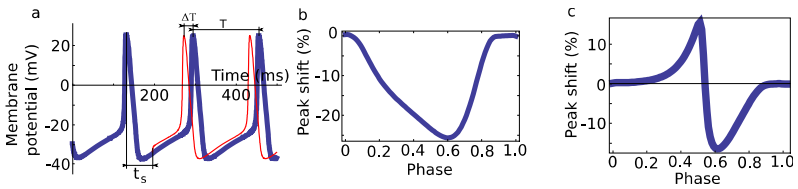

INTRODUCTION

Predicting the behavior of a single neuron has been a focus of neuroscience for more than a century.[1,2] To make predictions, scientists build models based on the study of the cause-effect relationship of selected natural phenomena; in our case, models that capture the mechanisms responsible for the observable neural behavior.

One of the most notorious mathematical model was derived around the 1950s by A. L. Hodgkin and A. F. Huxley, who published a series of papers describing a realistic model of APs in giant squid axons.[3] The conductance-based Hodgkin- Huxley (HH) model was based on experiments that started in the 1930s and stopped because of the Second World War. Later, C. Morris and H. Lecar used the giant barnacle muscle fiber to model neuronal oscillatory phenomena with a reduced, two-variable, system of equations.[4,5] Remarkable modeling procuresses were made by Connor, who discovered the mechanism of repetitive neuronal firing,[6] Hindmarsh and Rose, who modeled bursting activity.[7] Finally, the Fitz Hugh and Nagumo model offered a general method for reducing the complexity of HH-type models.[8,9]

Biophysically realistic models can reveal intricate nonlinear couplings among variables that could be difficult to isolate in a wet experiment. A model can also be used as substitute for physical experimentation when the latter would prove too challenging, too expensive, or ethically problematic.[10]

* Corresponding author:

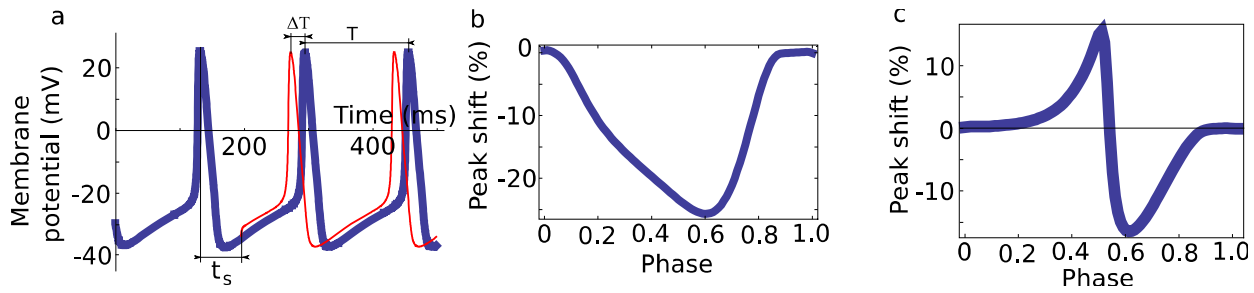

Fig. 1 – (a) The thick (blue) curve is the unperturbed membrane voltage of a periodically spiking neuron. The thinner (red) curve is the membrane potential after a brief stimulus perturbs the cell cycle at t_s relative to the most recent AP. The change in the intrinsic firing period T due to the external stimulus is ΔT. (b) The peak shift ΔT relative to the intrinsic firing period T for Type I PRCs is usually unimodal, and (c) for Type II PRCs is bimodal.

In this study, we used a single-compartment HH type model and the method of Phase Resetting Curves (PRCs) to uncover the effect of presynaptic stimuli on the stereotypical shape of APs.

Clock-like rhythms are ubiquitous phenomena. The rhythmic nature of our environment has primed living organisms to exhibit rhythmic patterns of activity.[11] Biological rhythms vary from the circadian rhythms to cell divisions to the firing pattern of oscillatory neurons. The mechanisms that govern biological cycles are, in essence, biochemical, and the underlying principles that govern their action can be mathematically and computationally described in great detail.[12] Furthermore, these repeating patterns can be studied on different levels, from the organism (or behavioral) to the network (aggregation of cells) down to the single-cell level and even a genetic level. In this study, we focus on the single-cell level modeling.

Any spiking neuron can be modeled as a limit cycle oscillator, a system in which all biophysically relevant variables, such as the membrane potential, have the same value as they had at the same phase of the previous cycle of activity (see Fig. 1a thick blue curve).[13] A stimulus perturbs the intrinsic firing rate of the cell, inducing a transient shift in its firing period T (see the thin red curve in Fig. 1a). The transient change of the firing pattern is determined by the stimulus timing t_s relative to the most recent AP.[14] We often use the stimulus phase as the normalized stimulus time t_s relative to the intrinsic firing period T, *i.e.*, $phase = t_s/T$. A PRC is a quantitative measure of the normalized AP peak shift $\Delta T/T$ that a particular perturbation induces on the timing of the next spike (see Fig. 1).[15]

Notice in Fig. 1a that the time difference ΔT does not change if there is no further stimulation. This shows that the induced change in period ΔT was transient, *i.e.*, the neuron returns to its intrinsic firing period T. An infinitesimal PRC tabulates the normalized period shifts $\Delta T/T$ induced by stimuli with infinitely small durations.[16,17] A more biologically realistic representation of phase response tabulates the relative changes of the period $\Delta T/T$ induced by a finite-duration stimulus.[17-19] In our case, one firing period was split into 200 equally spaced phase intervals. At the beginning of the first phase interval, a stimulus is injected at stimulus time $t_s = 0$ (Fig. 1a), and the normalized change in the period $\Delta T/T$ is recorded. Then the simulation is injected into the next phase interval and so on (see Fig. 1b and Fig. 1c).

The PRCs have been used to study how the coupling of neurons influences their relative firing phase in neural networks.[20,21]

We can distinguish among different types of neural oscillators according to three criteria: excitability class, bifurcation diagram, and PRC type.[22] Hodgkin and Huxley introduced excitability classes based on the relationship between the firing frequency and the bias current. In a nutshell, Class I neurons do not have a limited frequency response, whereas Class II neurons do.[23] The third class describes non-oscillatory neurons and will not be discussed here. Later, bifurcation diagrams added the stability analysis to the excitability classification.[24,25] Class I excitability emerges from a saddle-node bifurcation, whereas Class II exhibits a Hopf bifurcation.[5] We can also distinguish Type I and Type II neural oscillators based on their PRC. For example, PRCs for Type I oscillators are unimodal (Fig. 1b), and Type II neurons have a bimodal PRC (Fig. 1c). It so happened that neurons exhibiting a saddle-node bifurcation diagram yielded unimodal PRCs, *i.e.*, Type I neural oscillators, and correspond to HH Class I continuous excitability. Similarly, systems characterized by Hopf bifurcation diagrams lead to Type II PRCs and also belong to Class II

excitability. However, we must also mention that there are exceptions to this clear-cut picture. For example, it has been recently discovered that in some cases, saddle-node diagrams neurons yield PRCs with strong bimodal characteristics.[16] Additionally, it was shown that all PRCs have bimodal characteristics. However, it looks like Type I PRCs are unimodal because one lobe of the bimodal response is tiny compared to the other. Thus, bimodality is, in fact, due to the existence of both saddle-node and Hopf bifurcation.[26]

METHODS

The detailed mathematical model is presented in the Appendix. Integrating the model's equations, one gets the steady unperturbed firing pattern of oscillatory neurons (not shown). The firing period can be changed by changing the bias (rheobase) current (see Appendix).

Our goal was to investigate the effect of different stimulus characteristics on neurons responses. For example, what is the model neuron sensitive to, and what changes can be recorded in its response? We carried out two sets of numerical experiments.

Experiment 1: we used a rectangular stimulus (Fig. 2a) and examined the responses of the neural model to changes in amplitude A and duration δt of the stimulus (Fig. 2c).

Experiment 2: we used a triangular pulse (Fig. 2b) to investigate the influence of the amount of electric charge injected into the neuron. A widely accepted tenet in neuroscience is that the characteristics of the stimulus that governs the response of a neuron is the area under the curve of a particular stimulus, *i.e.*, the electric charge injected into the cell. For Experiment 2, all stimuli have the same amplitude A, duration δt, and phase of injection. Hence their area, *i.e.*, the injected electric charge is the same. However, the triangle's peak was moved relative to the start of the stimulus to change its shape without changing its area, *i.e.*, the amount of electric charge injected.

A PRC quantifies the phase-dependent effects that a particular stimulus $(A,\delta t)$ has on the period of an oscillatory neuron. How can we use the PRC to compare the effects that different stimuli have on a neuron? Experimental data showed that external stimuli have two main influences on the PRC: (1) change its peak-to-peak amplitude and (2) circularly shift the PRC. It seems that the overall shape of the PRC remains unchanged. We can compare two PRCs by using the following scaling relationship

$$\mathrm{PRC}_2 = \alpha\,\mathrm{PRC}_1 + \beta,$$

where α is a scale factor determined by the peak-to-peak ratio of PRC amplitudes, and β represents the horizontal shift of the PRCs with respect to each other (Fig. 2 c). The scale coefficients (α, β) compare the effect of different stimuli over the entire phase range and show that these differences are consistent independently of the phase.

RESULTS

Experiment 1: rectangular pulses of variable amplitudes A and durations δt. As we increased the stimulus current amplitude A, we obtained PRCs with larger amplitude, *i.e.*, larger ratio α, but no horizontal shift β (Fig. 3a). The relationship between the amplitude A of the rectangular stimulus (Fig. 2a) and the change in the firing period induced was linear, *e.g.*, if we double the amplitude of the stimulus, we double the amplitude of the PRC.

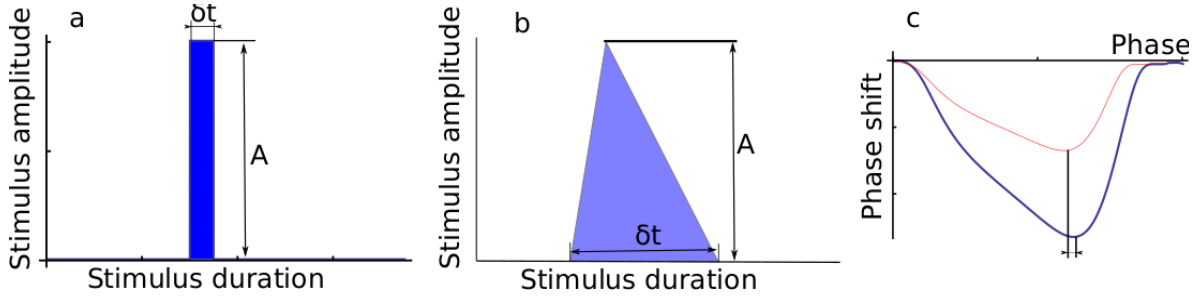

Fig. 2 – (a) Rectangular and (triangular) stimuli have two effects on the PRC (c): a change in amplitude and a horizontal shift of the PRC peak. The (blue) thick PRC is in response to a rectangular stimulus $(A,\delta t)$ of the same duration as for the (red) thin PRC but double amplitude, *i.e.*, $(2A, \delta t)$.

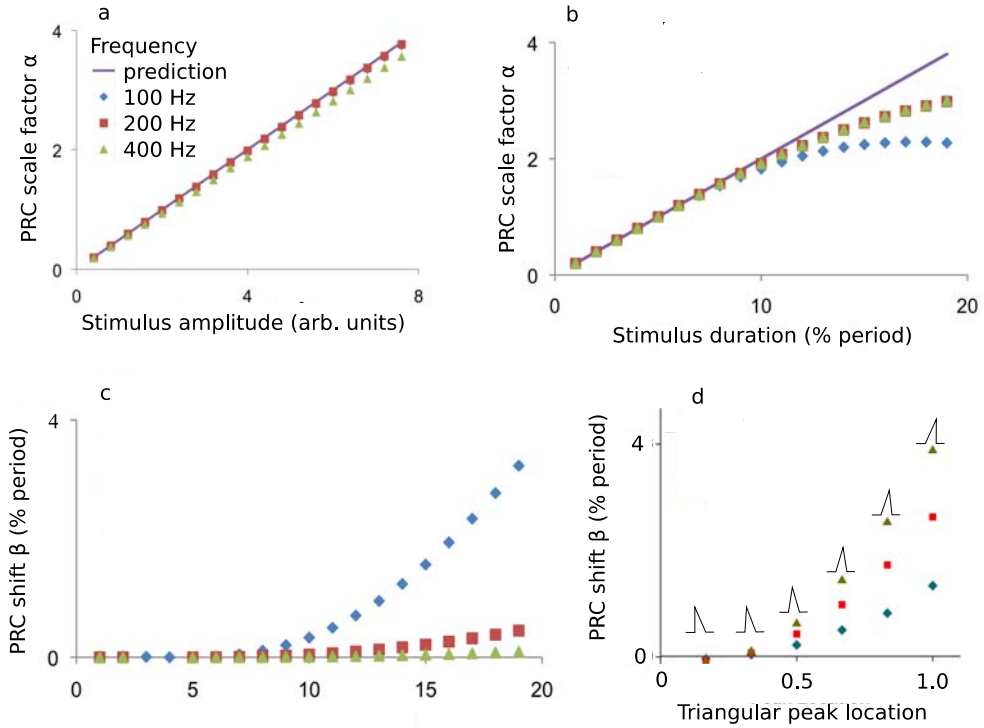

Fig. 3 – (a) The scaling factor α for the amplitude of the PRC linearly increases with the rectangular stimulus amplitude A. The slope of the linear relationship is almost the same regardless of the neuron's frequency. (b) The duration δt of the rectangular stimulus has a nonlinear contribution to the scale factor α of the PRC. (c) The PRC horizontal shift β increases exponentially with rectangular stimulus duration δt. The shift β becomes significant when the duration exceeds 10 percent of the intrinsic period T. (d) The PRC shift β is significant for triangular pulses with the same area (the same net electric charged injected) but with different shapes. The peak shift also increases with the spiking frequency.

In Fig. 3, the continuous line represents what we would expect if there is a positive linear correlation between the change in period ΔT and the amplitude A of the rectangular stimulus (Fig. 3a). Changes in stimulus duration δt induce nonlinear responses (Fig. 3b). This effect is most significant when the stimulus duration exceeds 10 percent of the intrinsic period T. The nonlinear effect of stimulus duration manifests stronger at higher frequencies (Fig. 3b). Changes in stimulus duration δt also induce horizontal shifts β that we did not observe for changes in stimulus amplitude A (Fig. 3c). To summarize, in Experiment 1, we found that the neuron responds linearly to changes in stimulus amplitude (Fig. 3a) but non-linearly to changes in duration (Fig 3b and 3c). These findings raise the question of whether the response depends only on the amount of electric charge injected into the neuron for a particular phase. The electric charge injected equals the area under the curve of a stimulus current versus time. Assuming that the neuron is only sensitive to the amount of injected electric charge, we would expect that it responds linearly to the stimulus area, which is proportional to the product between the amplitude A and duration δt. Based on the observed asymmetry between the response of neurons to stimulus amplitude A and duration δt found in Experiment 1, we hypothesized that even the shape of the stimulus, not just the total area (electric charge) of the stimulus, is essential for neural communication. To test our hypothesis, we injected triangular pulses (Fig. 2b). We kept the same duration δt and the amplitude A for all triangular pulses. The only variable was the peak location of the triangle related to the start of the stimulus (Fig. 3d). We found that injecting triangular stimuli with the same total area but different peak locations yielded PRCs with the same amplitudes (not shown). However, we determined that the shape of the stimulus produces a significant horizontal shift of the PRC (Fig. 3d).

CONCLUSIONS

There is extensive literature regarding the resetting effect that stimuli have on the firing period of neurons. It is generally accepted that neurons encode information by changing their

firing frequency. Our results show that neural information processing is more complex than previously thought. Neurons are sensitive to the electric charge (total area of the stimulus) and the phase of stimuli. We found that neurons also encode information regarding the shape of the input stimuli. Because neurons can discriminate between different shapes of pre-synaptic potentials, and because the shape of the pre-synaptic input modulates not only the timing but the shape of post-synaptic potentials, then the principle that neurons encode information strictly by modulating their firing rate is incomplete.

In all experiments carried out here, the neuron's response to stimuli increases as the neuron's firing frequency increases. Thus, a stimulus of the same amplitude or duration injected at the same phase will significantly affect a neuron with a shorter period. This is due to the relative ratio between the intrinsic firing period of the neuron and the stimulus duration. The injected charge's absolute value alone is not the crucial variable.

Acknowledgments. This research was supported by a Research and Development grant from the College of Charleston and an award from the South Carolina Space Grant Consortium. Support was also provided by grants from the National Center for Research Resources (5 P20 RR016461) and the National Institute of General Medical Sciences (8 P20 GM103499) from the National Institutes of Health.

APPENDIX -MATHEMATICAL MODEL

Our model was inspired by M. Pospichil *et al*.,[27] which is a single-compartment HH model modified to simulate cortical neurons. The following equation governs the membrane potential:

$$C_m\, dV/dt = - I_{Na} - I_K - I_L + I_{bias},$$

where V is the membrane potential, C_m is the membrane capacitance in μF/cm^2. I_{Na} is the voltage-dependent sodium current, and I_K is the delayed rectifier potassium current. I_L is the leak current, and I_{bias} is the bias current, or rheobase, that controls the firing frequency of the neuron. The sodium and potassium currents were fitted for central cortical neurons by Traub and Miles.[28] The sodium current is represented by

$$I_{Na} = g_{Na}\, m_{Na}^3\, h_{Na}\, (V - E_{Na}),$$

where g_{Na} = 100 mS/cm^2 the maximal sodium conductance, m_{Na} and h_{Na} are the activation and inactivation variables, and E_{Na} = 50 mV is the Nernst potential for sodium. The activation function was

$$dm/dt = \alpha_m(V)(1 - m) - \beta_m(V)\, m,$$

where $\alpha_m = (-0.32\,(V - V_t - 13))/(e^{-(V-V_t-13)/4}-1)$, $\beta_m = (0.28(V - V_t - 40))/(e^{-(V - V_t - 40)/5}-1)$.

The inactivation function was defined as

$$dh/dt = \alpha_h(V)(1 - h) - \beta_h(V)\, h,$$

where $\alpha_h = 1.128\, e^{-(V-V_t-17)/18}$, $\beta_h = 4/(1+e^{-(V - V_t - 40)/5})$. V_t = -56.2 mV adjusts the spike threshold.

The potassium current is

$$I_K = g_K\, n^4\, (V - E_K),$$

where g_K = 10 mS/cm^2 is the maximal potassium conductance, n is the fraction of potassium channels open, and E_K = -90 mV is the Nernst potential for potassium. n was defined as

$$dn/dt = \alpha_n(V)(1 - n) - \beta_n(V)\, n,$$

where $\alpha_n = (-0.032(V - V_t - 15))/(e^{-(V-V_t-15)/5}-1)$, $\beta_n = 0.5\, e^{-(V - V_t -10)/40}$.

The leak current was represented by $I_L = g_L\,(V - E_L)$, where g_L = 0.3 mS/cm^2 is the leak conductance of the membrane, and E_L = -54.4 mV is the reversal potential. The system's initial conditions are random, with the membrane voltage located between -75 mV and -55 mV. The oscillations are irregular initially and need to fire a couple of APs before entering a stable firing pattern. For this reason, we let the code run for over 1000 ms without perturbation.

REFERENCES

1. L. Abbott, *Brain Research Bull*., **1999**, *50*, 303-304.
2. L. Lapicque, *J. Physiol. Pathol. Gen.*, **1907**, *9*, 620-635.
3. A. L. Hodgkin and A. F. Huxley, *J. Physiol*, **1952**, *117*, 500-544.
4. C. Morris and H. Lecar, *Biophys. J.*, **1981**, *35*, 193-213.
5. K. Tsumoto, H. Kitajima, T. Yoshonaga, K. Aihara and H. Kawakami, *Neurocomputing*, **2006**, *69*, 293-316.
6. J. A. Connor, D. Walter and R. McKown, *Biophys J.*, **1977**, *18*, 81-102.
7. J. L. Hindmarsh, R. M. Rose and A. F. Huxley, *Proceed. Royal Soc. London, Series B., Biol. Sci.*, **1984**. *221*, 87-102.
8. R. Fitz Hugh, *Biophys. J.*, **1961**., *1*, 445-466.
9. J. Nagumo, S. Arimoto and S. Yoshizawa, *Proceed. IRE*, **1962**, *50*, 2061-2070.
10. R. R. Cisi and A. F. Kohn, *J. Comput. Neurosci.*, **2008**, *25*, 520-542.
11. V. K. Sharma, *Chronobiol. Int.*, **2003**, *20*, 901-19.
12. A. Winfree, "The geometry of biological time", 1980.
13. S. A. Oprisan, "A Geometric Approach to Phase Resetting Estimation Based on Mapping Temporal to Geometric Phase", in "Phase Response Curves in Neuroscience: Theory, Experiment, and Analysis", N. W. Schultheiss, A. A. Prinz and R. J. Butera (Eds.), Springer New York: New York, 2012, p. 131-162.

14. W. Govaerts and B. Sautois, *Neural Comput*., **2006**, *18*, 817-847.
15. S. A. Oprisan and C. C. Canavier, *Neural Comput.*, **2002,** *14*, 1027–1057.
16. G. B. Ermentrout, *Physica D: Nonlinear Phenomena*, **1990**, *41*, 219-231.
17. B. Ermentrout, *Neural Comput.*, **1996**, *8*, 979-1001.
18. C. C. Canavier, R.J. Butera, R.O. Dror, D.A. Baxter, J.W. Clark and J.R. Byrne, *Biol. Cybern.*, **1997**, *77*, 367-80.
19. S. A. Oprisan, A. A. Prinz and C. C. Canavier, *Biophys. J.*, **2004**, *87*, 2283-2298.
20. C. C. Canavier and S. Achuthan, *Math. Biosci.*, **2010**, *226*, 77-96.
21. A. Guillamon and G. Huguet, *SIAM J. Applied Dynamical Systems*, **2009**, *8*, 1005-1042.
22. S. A. Oprisan, *Neural Comput.*, **2014**, *26*, 132-157.
23. T. Yu, T. J. Sejnowski and G. Cauwenberghs, *IEEE Trans. Biomed. Circuits Syst.*, **2011**, *5*, 420-429.
24. A. Wagemakers, M.A.F. Sanjuan, J.M. Casedo and K. Aihara, *Int. J. Bifurcation and Chaos*, **2006**, *16*, 3617-3630.
25. S. Binczak, S. Jacquir, J.-M Bilbault, V.B. Kazantsev and V.I. Nekorkin, *Neural Netw*., **2006**, *19*, 684-693.
26. S. A. Oprisan, *ISRN Comput. Biol.*, **2013**, 230571.
27. M. Pospischil, M. Toledo-Rodriguez, C. Monier, Z. Piwkowska, T. Bal, Y. Fregnac, H. Markrom and A. Destexhe, *Biol. Cybernetics*, **2008,** *99*, 427-441.
28. R. D. Traub and R. Miles, "Neuronal Networks of the Hippocampus", Cambridge: Cambridge University Press, 1991.